Transmission-Line Coupled Reconfigurable Intelligent Surfaces Under Partial Illumination

Keisuke Konno, *Senior member, IEEE,* Keita Umemoto *Nonmember, IEEE,*, Takamasa Sato *Nonmember, IEEE,*, Qiang Chen, *Senior Member, IEEE* and Gabriele Gradoni *Member, IEEE*

***Abstract*—This work proposes a reconfigurable intelligent surface (RIS) coupled to a two-wire parallel transmission line and applies it to the partial-illumination problem. The RIS consists of dipole elements positioned on the receiving and transmitting sides of the transmission line. Incident power collected by illuminated dipoles is conveyed to unilluminated elements through transverse electromagnetic (TEM) waves supported by the transmission line, enabling beamforming even when part of the aperture is shadowed by a nearby scatterer. A coupling-coefficient-based geometric optimization and a load-reactance optimization derived from the method of moments (MoM) are employed to control the aperture distribution and steer the main beam. Numerical simulations demonstrate (i) enhanced excitation of shadowed RIS elements and (ii) beam scanning behind the scatterer with a scattering-field improvement of approximately 4–7 dB. These results confirm that transmission-line coupling effectively mitigates partial illumination in RIS-based beamforming systems.**

***Index Terms*—Reconfigurable intelligent surface, transmission line, partial illumination, beam scanning, mutual coupling.**

I. Introduction

PLANAR reflectarrays provide a low-profile alternative to conventional reflector antennas and have been widely applied in satellite communications, imaging, and beamforming systems [1]–[8]. Although various approaches have been proposed for designing the aperture distribution of the planar reflectarrays, beam steering away from broadside is limited by the reduction in effective aperture with increasing scan angle [9]–[12]. Passive repeater and dual-antenna concepts partially address this limitation by transferring received power between orthogonal apertures via transmission lines [13]- [15].

Recent guided-wave-assisted RIS architectures—including wave-controlled metasurfaces and surface-wave-coupled apertures—demonstrate improved beam manipulation [16]- [20]. Nevertheless, prior studies typically neglect partial illumination caused by nearby scatterers, which reduces the number of effectively excited RIS elements and degrades beam-steering capability. A beyond diagonal RIS (BD-RIS), which has been proposed to break through the limitation of conventional RIS, can also suffer from such partial illumination problem [21]–[23]. Prior studies have implied that performance of the BD-RIS such as channel gain can be enhanced with the help of mutual coupling [24], [25]. However, these studies have not discussed the physical structures of RIS that would enhance inter-element mutual coupling under a partial illumination environment. Moreover, these studies have not addressed to what extent mutual coupling can improve the aperture field distribution or the beam-scanning performance of the RIS under a partial illumination environment. In addition to these works, various modeling on RIS including effect of mutual coupling has also been proposed but they have not addressed the partial illumination problem [26]–[28].

This paper introduces a two-wire-transmission-line-coupled RIS that maintains excitation of shadowed elements via TEM-wave coupling. The main contributions are:

1) Demonstration of tunable aperture distribution in the presence of a scatterer through coupling-coefficient optimization.
2) Proof of beam scanning behind the scatterer enabled by transmission-line-mediated excitation of unilluminated elements.

This letter is organized as follows. Geometry and coupling mechanism of the proposed RIS is described in section II. In section II, length of RIS elements and width of the two-wire parallel transmission line are numerically optimized from the viewpoint of a coupling coefficient. The variable load impedances of the proposed RIS is optimized and radiation performance of the optimized RIS is demonstrated in section III. Finally, this paper is concluded in section IV.

In this letter, definition of "reflectarray" is "array of multiple passive scatterers whose reflected beam is designed under specific intention". Also, definition of "RIS" is "array of multiple reconfigurable scatterers whose scattering performance such as main beam direction is tunable". This letter addresses both because they have a lot in common: array of multiple scatterers, application to coverage enhancement, [29], [30].

II. Geometry and Coupling Mechanism

A. Structure

The proposed RIS comprises a linear array of dipole elements above a reflecting plane, with variable load impedances placed at dipole centers to control radiation. A two-wire parallel transmission line located between the dipoles and the reflecting plane enables strong inter-element coupling through

K. Konno, K. Umemoto, T. Sato and Q. Chen are with the Department of Communications Engineering, Graduate School of Engineering, Tohoku University, Japan (*K. Konno and K. Umemoto contributed equally to this work. Corresponding author: Keisuke Konno*, e-mail:keisuke.konno.b5@tohoku.ac.jp).

K. Konno and G. Gradoni are with the 6G Innovation Center, Institute for Communication Systems, University of Surrey, Guildford, U.K and G. Gradoni is also with the Department of Computer Science and Technology, University of Cambridge, Cambridge, U.K (e-mail: g.gradoni@surrey.ac.uk).

This research was partly supported by Tohoku University Young Leaders Overseas Program and JSPS KAKENHI 26K00940.

Manuscript received August 25, 2011; revised March 29, 2012.

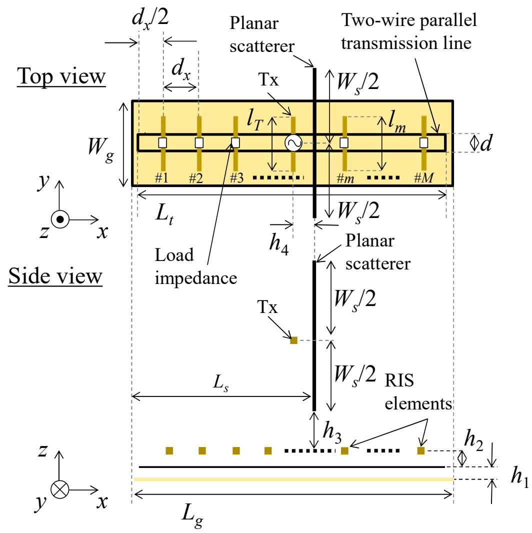

Fig. 1. Geometry of the proposed RIS.

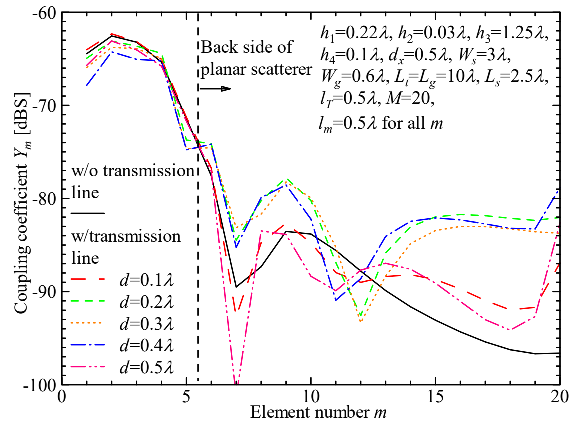

Fig. 2. Coupling coefficient of the proposed RIS elements (Here, l_m is length of mth dipole element and d is spacing between the transmission lines. $l_m = 0.5\lambda$ for all m).

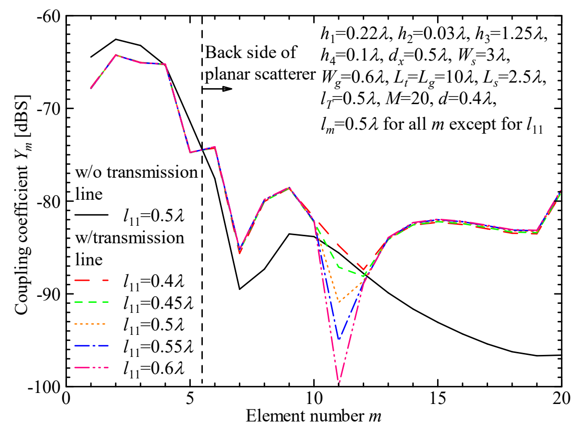

Fig. 3. Coupling coefficient of the proposed RIS elements (Here, l_m is length of mth dipole element and d is spacing between the transmission lines. $l_m = 0.5\lambda$ for all m except for l_{11}).

TEM waves. The proposed RIS is inspired by near-field fed traveling wave array antennas but is designed here as spatially illuminated coupled array via standing-wave [31]–[33]. The geometry and parameter definitions are illustrated in Fig. 1, where the transmission line links illuminated and shadowed dipoles across the scatterer. Illuminated dipoles receive power from a transmitting antenna and excite the two-wire parallel transmission line via y-polarized wave. On the excited (and short-circuited) two-wire parallel transmission line, standing waves appear because of superposition of incident/reflecting TEM waves. Shadowed dipoles, that are not well-excited by spatial illumination by the transmitting antenna, are excited by guided TEM wave on the two-wire parallel transmission line. Finally, the shadowed dipoles are well-excited and main beam tunability of the proposed RIS behind the scatterer is expected to be enhanced. In a realistic scenario, part of the line-of-sight path among the transmitting/receiving antennas and RIS elements can be blocked by an obstacle. Fig. 1 corresponds to such realistic scenario and far field radiation from RIS under partial illumination is modeled. Numerical results in this paper are obtained in the presence of the scatterer.

B. Coupling Coefficient

To quantify transmission-line-mediated excitation, the coupling coefficient is defined as

$$Y_m = \frac{I_m}{V_t} \tag{1}$$

where I_m is current at the center part of the mth RIS elements and V_t is excitation voltage of the transmitting dipole antenna.

Examples of simulated coupling coefficients Y_m are shown in Fig. 2. Here, numerical simulation was performed by method of moments (MoM) and our developed in-house code was used [34], [35]. During the numerical simulation, all the RIS elements are short-circuited. It is found that the coupling coefficients of the unilluminated RIS elements arranged behind the planar scatterer are enhanced by the two-wire parallel transmission line whereas they are small when the transmission line is absent. Except for specific RIS elements whose coupling coefficient drops by introducing the two-wire parallel transmission line, $3 \sim 18$ dB enhancement of the coupling coefficient is achieved for the RIS elements arranged behind the planar scatterer, approximately. As shown in Fig. 3, drop of the coupling coefficient by introducing the two-wire parallel transmission line can be enhanced once l_m is tuned locally. Finally, $l_m = 0.5\lambda$ for all m except for $l_{11} = 0.4\lambda$ and $d = 0.4\lambda$ are chosen as the best parameters here for enhancing amplitude of current distribution and for keeping its variation as small as possible. Current distribution of the RIS elements and the two-wire parallel transmission line is shown in Fig. 4. It is found that the RIS elements behind the planar scatterer cannot be excited well without the two-wire parallel transmission line whereas they can be excited well by introducing it. In particular, the current distribution of the five to six RIS elements farthest from the planar scatterer were enhanced by more than 10 dB. It clearly indicates that the transmission line contributes to enlarging the effective aperture of the RIS under the partial illumination problem. Also, the standing wave is excited on the two-wire parallel transmission line as expected.

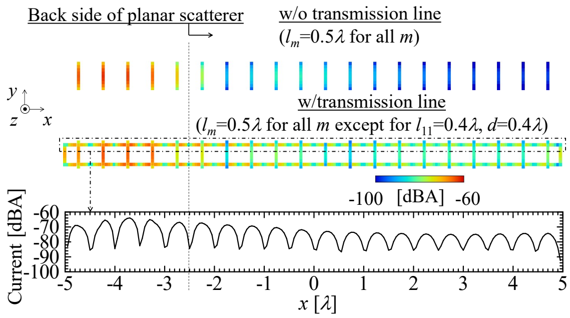

Fig. 4. Current distribution of the RIS elements and two-wire parallel transmission line (Here, l_m is length of mth dipole element and d is spacing between the transmission lines. Parameters except for l_m and d are the same as those in Fig. 3.).

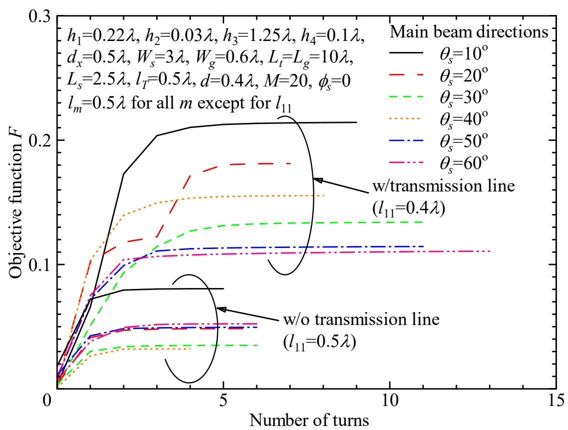

Fig. 5. Convergence of the optimization process. Here, the total number of RIS elements is $M = 20$. Therefore, single turn includes 20 times updates of variable load impedances. See appendix A for elaborated optimization process.

Enhancement and drop of the coupling coefficients by the two-wire parallel transmission line can be elaborated as follows. As shown in Fig. 2, the coupling coefficients of the shadowed RIS elements are non-zero even when the two-wire parallel transmission line is absent. The non-zero coupling coefficients come from mutual coupling between RIS elements or diffraction by the scatterer. Therefore, once the mutual coupling via TEM waves introduced by the two-wire parallel transmission line strengthens the originally existing mutual coupling, the coupling coefficients enhance and vice versa.

Discussions on simulated coupling-coefficient distributions here are summarized as follows:

1) w/o the transmission line, shadowed elements exhibit very weak excitation.
2) w/the transmission line, excitation increases by $3 \sim 18$ dB for elements behind the scatterer.
3) Local geometric tuning further stabilizes the current distribution.

The current distribution visualization in Fig. 4 confirms strong excitation of previously inactive elements and standing-wave formation along the transmission line. These observations indicate an effective enlargement of the RIS aperture under partial illumination.

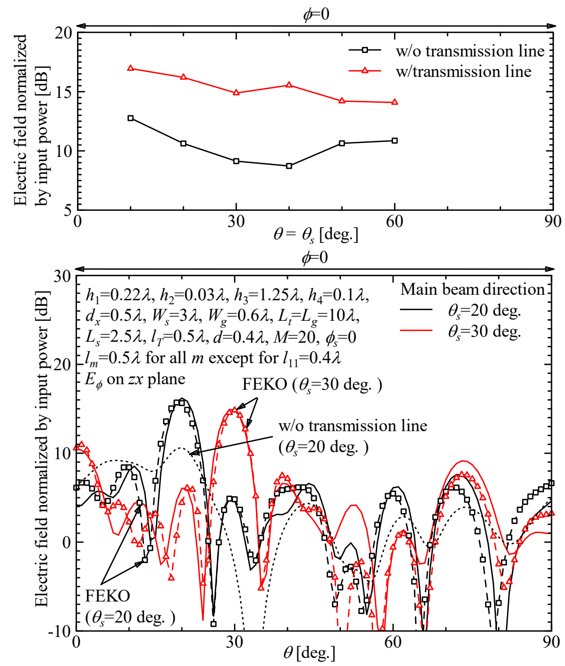

Fig. 6. Beam-scanning by the proposed RIS. Bottom one shows radiation patterns of the proposed RIS whereas top one shows envelope of main beam level of the RIS corresponding to different mainbeam directions ranging from $\theta_s = 10$ to 60 deg. For, $\theta_s = 30$ deg., load impedances corresponding to $m = 1 \sim 20$ are: -j2490, j40, -j239, -j12500, -j38, -j408, -j12300, j231, -j193, j13000, j108, -j5, -j205, -j1720, -j12800, j22, -j155, -j2660, j356, j135.

III. Beam Scanning Under Partial Illumination

A. Optimization Formulation

Here, beam scanning capability of the proposed RIS under a partial illumination environment is demonstrated. Variable load impedances (pure reactance) are optimized to maximize the following objective function

$$F = |E_\phi(\theta = \theta_s, \phi = \phi_s)|^2 \qquad (2)$$

using an MoM-based iterative update method proposed by Hirasawa [36], [37]. Here, θ_s and ϕ_s are zenith and azimuth angles corresponding to main beam direction of the proposed RIS. Flowchart of the method is elaborated in appendix A.

Fig. 5 shows convergence of the objective function during optimization. The convergence behavior in Fig. 5 shows rapid improvement of the objective function when the transmission line is included, with total optimization time below 90 sec. for current segments. Once the two-wire parallel transmission line is introduced, simulation model becomes large and resultant convergence is slow. Convergence to the local minimum is avoidable once the optimization starts from different initial values of load impedances. Here, numerical simulation was performed by a workstation with AMD Ryzen 9 9950X 16-Core Processor (32CPUs) (4.30 GHz) and the total number of current segments are $N = 5269$.

B. Beam Scanning Performance

Fig. 6 shows beam scanning performance of the RIS w/ or w/o two-wire parallel transmission line. According to Fig. 6, it is found that main beam level of the proposed RIS is

TABLE I
COMPARISON OF WAVEGUIDE COUPLED RIS.

Study	Waveguide & Coupling mechanism	w/ or w/o tunability	w/ or w/o obstacle
[17]	Metasurface, Surface wave	w/o	w/o
[18], [19]	Microstrip line, Standing wave	w/, biasing	w/o
[20]	Metasurface, Surface wave	w/, freq. scan	w/o
This work	Two-wire parallel transmission line, Standing wave	w/, variable load	w/

enhanced to the directions behind the scatterer because the shadowed RIS elements are excited by standing wave on the two-wire parallel transmission line. Owing to the two-wire parallel transmission line, it is found that $4 \sim 7$ dB enhancement of the scattering field is achievable.

Finally, discussions on radiation patterns shown in Fig. 6 are summarized as follows:

1) w/o transmission line: main beam is largely fixed, and its level is low because shadowed elements remain inactive.
2) w/transmission line: main beam is tunable behind the scatterer with $4 \sim 7$ dB radiation enhancement.

TABLE I summarizes contribution of this work over conventional works.

A couple of topics to be discussed remain: dielectric/conductor losses and bandwidth. In practice, dielectric/conductor losses, that are neglected in this letter, constrain the effective aperture size of the RIS that can be extended using the two-wire parallel transmission line, and reduce its efficiency. Therefore, low loss material is preferable for design and fabrication of the proposed RIS. Although numerical results were omitted due to limitation of pages, bandwidth of the proposed RIS was simulated by FEKO for $\theta_s = 30$ deg. @ 1 GHz, fractional 3-dB bandwidth is 3 %. Narrow bandwidth of the proposed RIS come from the optimization process at single frequency and optimization over specific frequency band is expected to enhance its bandwidth.

IV. CONCLUSION

In this letter, a transmission-line-coupled RIS has been presented to address the partial-illumination problem. Coupling-coefficient analysis and MoM-based optimization demonstrate:

1) Enhanced excitation of shadowed RIS elements.
2) Tunable aperture distribution in the presence of a scatterer.
3) Beam scanning behind the scatterer with measurable radiation-field enhancement.

These results establish guided-wave coupling via transmission lines as a practical mechanism for robust RIS beamforming in obstructed environments.

APPENDIX A
OPTIMIZATION METHOD

Flowchart of the optimization is as follows [36], [37].

1) According to the MoM formalism, RIS elements, reflecting plane, two-wire parallel transmission line, transmitting antenna, and scatterer are divided into N current segments. Resultant $N \times N$ matrix equation

$$\mathbf{V} = (\mathbf{Z}_{p-1} + \mathbf{Z}_p^L)\mathbf{I}_p \tag{3}$$

is numerically obtained. Here, $\mathbf{V}$ is known N dimensional voltage vector and $\mathbf{Z}_{p-1}$ is known $N \times N$ impedance matrix including variable load impedances updated by the $(p-1)$th iterations. $\mathbf{Z}_p^L = \mathrm{diag}(0, ..., Z_{qq}^L, ..., 0)$ is $N \times N$ diagonal load impedance matrix at the pth iterations and its entries are zero except for qqth component. $\mathbf{I}_p$ is unknown N dimensional current vector at the pth iterations. During optimization, variable load impedances Z_{qq}^L corresponding to central current segment of RIS elements is only updated and remaining ones are zero.

2) At the pth iteration, according to (3), $\mathbf{I}_p$ is obtained as follows.

$$(\mathbf{Z}_{p-1})^{-1}\mathbf{V} = (\mathbf{Z}_{p-1})^{-1}(\mathbf{Z}_{p-1} + \mathbf{Z}_p^L)\mathbf{I}_p \tag{4}$$

$$\mathbf{I}_{p-1} = (\mathbf{U} + (\mathbf{Z}_{p-1})^{-1}\mathbf{Z}_p^L)\mathbf{I}_p \tag{5}$$

Here, for the first iteration (i.e. $p = 1$), $\mathbf{Z}_{p-1} = \mathbf{Z}_0$ is known short-circuited $N \times N$ impedance matrix and $\mathbf{I}_{p-1} = \mathbf{I}_0$ is its N dimensional current vector. Therefore, both $\mathbf{I}_{p-1} (= (\mathbf{Z}_{p-1})^{-1}\mathbf{V})$ and $(\mathbf{Z}_{p-1})^{-1}$ are known at the pth iteration, recursively. $\mathbf{U}$ is $N \times N$ unit matrix. According to (5), each element of $\mathbf{I}_p = (I_1^{(p)}, I_2^{(p)}, ..., I_N^{(p)})$ is explicitly described as follows.

$$I_n^{(p)} = I_n^{(p-1)} - \frac{Z_{qq}^L Y_{nq}^{(p-1)} I_q^{(p-1)}}{1 + Z_{qq}^L Y_{qq}^{(p-1)}} \text{ where } n = 1, ..., N \tag{6}$$

Here, $Y_{nq}^{(p-1)}$ and $Y_{qq}^{(p-1)}$ are known nq and qq components of $(\mathbf{Z}_{p-1})^{-1}$, respectively.

3) (6) gives $\mathbf{I}_p$ as a single parameter function of Z_{qq}^L to be updated because remaining values are known and constant. Therefore, (2) is also expressed as a single parameter function of Z_{qq}^L, once $\mathbf{I}_p$ is substituted into (2). Brent method is used and Z_{qq}^L is obtained numerically so that (2) is maximized [38].
4) For the $(p+1)$th iteration, entries of $(\mathbf{Z}_{p-1})^{-1}$ are updated to $(\mathbf{Z}_p)^{-1}$ so that Z_{qq}^L is included. Sherman-Morrison formula is used to update entries of $(\mathbf{Z}_{p-1})^{-1}$ as follows [39].

$$Y_{nm}^{(p)} = Y_{nm}^{(p-1)} - \frac{Y_{nq}^{(p-1)} Y_{qm}^{(p-1)} Z_{qq}^L}{1 + Z_{qq}^L Y_{qq}^{(p-1)}}$$
$$\text{where} \quad n = 1, ..., N, \quad m = 1, ..., N \tag{7}$$

5) $2) \sim 4)$ are iterated until all M variable load impedances are updated once.
6) The next turn for further updating the variable load impedances starts unless F satisfy the following stopping criteria.

$$|F_p - F_{p-M}|/F_{p-M} < 10^{-3} \tag{8}$$

Here, F_p and F_{p-M} are objective functions at the end of this (i.e. $p = M, 2M, ...$) and previous turn, respectively.

REFERENCES

[1] J. Huang, "Analysis of a microstrip reflectarray antenna for microspacecraft applications," *TDA Progress Report* 42-120, Feb. 1995, pp. 153-173.

[2] J. Huang and J. A. Encinar, Reflectarray Antennas, *John Wiley and Sons*, 2008.

[3] D. G. Berry, R. G. Malech, and W. A. Kennedy, "The reflectarray antenna," *IEEE Trans. Antennas Propag.*, vol. 11, no. 6, pp.645-651, Nov. 1963.

[4] J. A. Encinar, and J. A. Zornoza, "Three-layer printed reflectarrays for contoured beam space applications," *IEEE Trans. Antennas Propag.*, vol. 52, no. 5, pp. 1138-1148, May 2004.

[5] J. A. Encinar, M. Arrebola, L. F. de la Fuente, and G. Toso, "A transmit-receive reflectarray antenna for direct broadcast satellite applications," *IEEE Trans. Antennas Propag.*, vol. 59, no. 9, pp. 3255-3264, Sept. 2011.

[6] M. Zhou, S. B. Sørensen, O. S. Kim, E. Jørgensen, P. Meincke, and O. Breinbjerg, "Direct optimization of printed reflectarrays for contoured beam satellite antenna applications," *IEEE Trans. Antennas Propag.*, vol. 61, no. 4, pp. 1995-2004, April 2013.

[7] R. Florencio, J. A. Encinar, R. R. Boix, V. Losada, and G. Toso, "Reflectarray antennas for dual polarization and broadband telecom satellite applications," *IEEE Trans. Antennas Propag.*, vol. 63, no. 4, pp. 1234-1246, April 2015.

[8] H. Kamoda, T. Iwasaki, J. Tsumochi, T. Kuki, and O. Hashimoto, "60-GHz electronically reconfigurable large reflectarray using single-bit phase shifters," *IEEE Trans. Antennas Propag.*, vol. 59, no. 7, pp. 2524-2531, July 2011.

[9] P. Nayeri, F. Yang and A. Z. Elsherbeni, "Design and experiment of a single-feed quad-beam reflectarray antenna," *IEEE Trans. Antennas Propag.*, vol. 60, no. 2, pp. 1166-1171, Feb. 2012.

[10] P. Nayeri, F. Yang and A. Z. Elsherbeni, "Design of single-feed reflectarray antennas with asymmetric multiple beams using the particle swarm optimization method," *IEEE Trans. Antennas Propag.*, vol. 61, no. 9, pp. 4598-4605, Sept. 2013.

[11] K. Konno and Q. Chen, "Enhancing aperture efficiency of reflectarray by accurately evaluating mutual coupling of reflectarray elements," *IEICE Commun. Express*, vol. 5, no. 9, pp.341-346, 2016.

[12] K. Konno and Q. Chen, "A study on scattering field performance of reflectarray element covered by dielectric superstrate," *IEEE Trans. Antennas Propag.*, vol. 70, no. 10, pp. 9305-9314, Oct. 2022.

[13] L. Wang, S.-W. Qu, J. Li, Q. Chen, Q. Yuan, and K. Sawaya, "Experimental investigation of MIMO performance using passive repeater in multipath environment," *IEEE Antennas Wireless Propag. Lett.*, vol. 10, pp. 752-755, 2011.

[14] S.-W. Qu, Q.-Y. Chen, Q. Chen, J. Li, Q. Yuan, and K. Sawaya, "Dual-antenna system composed of patch array and planar Yagi antenna for elimination of blindness in cellular mobile communications," *Prog. Electromagn. Res. C*, vol. 21, 87–97, 2011.

[15] Y. Takahashi and N. Honma, "Improving the propagation environment by using tunable passive repeater," *Electronics* vol. 7, no. 2, pp.1-11, 2018.

[16] E. Ayanoglu, F. Capolino and A. L. Swindlehurst, "Wave-controlled metasurface-based reconfigurable intelligent surfaces," *IEEE Wireless Commun.*, vol. 29, no. 4, pp. 86-92, August 2022.

[17] J. Budhu, "Near-perfect space-wave to surface-wave coupler enabled conformal space wave transporting metasurfaces," *IEEE Trans. Antennas Propag.*, vol. 72, no. 3, pp. 2540-2554, March 2024.

[18] G. B.-Itzhak, M. S.-Melo, B. Bradshaw, E. Ayanoglu, F. Capolino and A. L. Swindlehurst, "Design and operation principles of a wave-controlled reconfigurable intelligent surface," *IEEE Open J. Commun. Soc.*, vol. 5, pp. 7730-7751, 2024.

[19] B. Bradshaw, M. Saavedra-Melo and F. Capolino, "Wave-controlled RIS: Biasing RIS elements using standing waves with single frequency," *Proc. EuCAP2025*, pp.1-4, 2025.

[20] T. Arshed, S. Maci and E. Martini, "Surface-wave metaprism for smart surface communications," *IEEE Trans. Antennas Propag.*, vol. 73, no. 9, pp. 6535-6545, Sept. 2025.

[21] M. Nerini and B. Clerckx, "Physically consistent modeling of stacked intelligent metasurfaces implemented with beyond diagonal RIS," *IEEE Commun. Lett.*, vol. 28, no. 7, pp. 1693-1697, July 2024.

[22] J. Tapie, M. Nerini, B. Clerckx and P. d. Hougne, "Beyond-diagonal RIS prototype and performance evaluation," *IEEE Wireless Commun. Lett.*, vol. 15, pp. 1-5, 2026.

[23] A. Azarbahram, O. L. A. López, B. Clerckx, M. Di Renzo and M. Latva-Aho, "Beamforming and waveform optimization for RF wireless power transfer with beyond diagonal reconfigurable intelligent surfaces," *IEEE Trans. Wireless Commun.*, vol. 25, pp. 8826-8842, 2026.

[24] H. Li, S. Shen, M. Nerini, M. Di Renzo and B. Clerckx, "Beyond diagonal reconfigurable intelligent surfaces with mutual coupling: modeling and optimization," *IEEE Commun. Lett.*, vol. 28, no. 4, pp. 937-941, April 2024.

[25] M. Nerini, H. Li and B. Clerckx, "Global optimal closed-form solutions for intelligent surfaces with mutual coupling: Is mutual coupling detrimental or beneficial?," *IEEE Trans. Wireless Commun.*, vol. 25, pp. 3201-3214, 2026.

[26] K. Konno, S. Terranova, Q. Chen and G. Gradoni, "Generalized impedance model of wireless links assisted by reconfigurable intelligent surfaces," *IEEE Trans. Antennas Propag.*, vol. 72, no. 10, pp. 7691-7699, Oct. 2024.

[27] P. Mursia, F. Devoti, M. Rossanese, V. Sciancalepore, G. Gradoni, and M.D. Renzo, "T3DRIS: advancing conformal RIS design through in-depth analysis of mutual coupling effects," *IEEE Trans. Commun.*, vol. 73, no. 2, pp. 889-903, Feb. 2025.

[28] M. Nerini, G. Gradoni and B. Clerckx, "Physics-compliant modeling and scaling laws of multi-RIS aided MIMO systems," *IEEE Trans. Wireless Commun.*, vol. 25, pp. 6745-6759, 2026.

[29] L. Li, Q. Chen, Q. Yuan, K. Sawaya, T. Maruyama, T. Furuno, and S. Uebayashi, "Novel broadband planar reflectarray with parasitic dipoles for wireless communication applications," *IEEE Antennas Wireless Propag. Lett.*, vol. 8, pp. 881-885, 2009.

[30] L. Li, Q. Chen, Q. Yuan, K. Sawaya, T. Maruyama, T. Furuno, and S. Uebayashi, "Frequency selective reflectarray using crossed-dipole elements with square loops for wireless communication applications," *IEEE Trans. Antennas Propag.*, vol. 59, no. 1, pp. 89-99, Jan. 2011.

[31] C. J. Sletten, F. S. Holt, P. Blacksmith, Jr., G. R. Forbes, Jr., L. F. Shodin, and H. J. Henkel, "A new satellite tracking antenna," *WESCON/57 Conference Record*, vol. 1, pp.244,-261, Aug. 1957.

[32] K. Konno, K. Takeda, and Q. Chen, "Beam scanning capability and suppression of endfire radiation of dipole array antennas coupled to two-wire transmission line," *IEICE Commun. Express*, vol. 4, no. 12, pp.358-362, 2015.

[33] K. Konno, T. Sekiguchi, H. Sato, and Q. Chen, "Continuous mechanical beam scanning dipole array antenna coupled with meander two-wire parallel transmission line," *IEICE Commun. Express*, vol. 6, no. 8, pp.490-495, 2017.

[34] J. H. Richmond and N. H. Geary, "Mutual impedance of nonplanar-skew sinusoidal dipoles," *IEEE Trans. Antennas Propag.*, vol. AP-23, no. 3, pp. 412-414, May 1975.

[35] C. W. Chuang, J. H. Richmond, N. Wang, and P. H. Pathak, "New expressions for mutual impedance of nonplanar-skew sinusoidal monopoles," *IEEE Trans. Antennas Propag.*, vol. 38, no. 2, pp. 275-276, Feb. 1990.

[36] K. Hirasawa, "Design of arbitrary shaped thin wire antennas by passive impedance loadings," *IEICE Trans. B*, vol. J61-B, no. 8, pp. 713-720, Aug. 1978 (in Japanese).

[37] K. Hirasawa, "Reduction of radar cross section by multiple passive impedance loadings," *IEEE J. Ocean. Eng.*, vol. 12, no. 2, pp. 453-457, April 1987.

[38] R. P. Brent, "Algorithms for minimization without derivatives," Courier Corporation, 2013.

[39] J. Sherman and W. J. Morrison, "Adjustment of an inverse matrix corresponding to a change in one element of a given matrix," *Ann. Math. Statist.* 21 (1) 124-127, March, 1950.